

SINCERE: Sequential Interaction Networks representation learning on Co-Evolving Riemannian manifolds

Junda Ye
Beijing University of Posts and
Telecommunications
Beijing, China
jundaye@bupt.edu.cn

Zhongbao Zhang
Beijing University of Posts and
Telecommunications
Beijing, China
zhongbaozb@bupt.edu.cn

Li Sun
North China Electric Power
University
Beijing, China
ccesunli@ncepu.edu.cn

Yang Yan
Beijing University of Posts and
Telecommunications
Beijing, China
yanyang42@bupt.edu.cn

Feiyang Wang
Beijing University of Posts and
Telecommunications
Beijing, China
fywang@bupt.edu.cn

Fuxin Ren
Beijing University of Posts and
Telecommunications
Beijing, China
renfuxin@bupt.edu.cn

ABSTRACT

Sequential interaction networks (SIN) have been commonly adopted in many applications such as recommendation systems, search engines and social networks to describe the mutual influence between users and items/products. Efforts on representing SIN are mainly focused on capturing the dynamics of networks in Euclidean space, and recently plenty of work has extended to hyperbolic geometry for implicit hierarchical learning. Previous approaches which learn the embedding trajectories of users and items achieve promising results. However, there are still a range of fundamental issues remaining open. For example, is it appropriate to place user and item nodes in one identical space regardless of their inherent discrepancy? Instead of residing in a single fixed curvature space, how will the representation spaces evolve when new interaction occurs?

To explore these implication for sequential interaction networks, we propose **SINCERE**, a novel method representing **Sequential Interaction Networks on Co-Evolving Riemannian manifolds**. SINCERE not only takes the user and item embedding trajectories in respective spaces into account, but also emphasizes on the space evolution that how curvature changes over time. Specifically, we introduce a fresh cross-geometry aggregation which allows us to propagate information across different Riemannian manifolds without breaking conformal invariance, and a curvature estimator which is delicately designed to predict global curvatures effectively according to current local Ricci curvatures. Extensive experiments on several real-world datasets demonstrate the promising performance of SINCERE over the state-of-the-art sequential interaction prediction methods.

Contact Junda Ye (jundaye@bupt.edu.cn) and Li Sun (ccesunli@ncepu.edu.cn) for any question.

Permission to make digital or hard copies of all or part of this work for personal or classroom use is granted without fee provided that copies are not made or distributed for profit or commercial advantage and that copies bear this notice and the full citation on the first page. Copyrights for components of this work owned by others than the author(s) must be honored. Abstracting with credit is permitted. To copy otherwise, or republish, to post on servers or to redistribute to lists, requires prior specific permission and/or a fee. Request permissions from permissions@acm.org.

WWW '23, May 1–5, 2023, Austin, TX, USA

© 2023 Copyright held by the owner/author(s). Publication rights licensed to ACM.
ACM ISBN 978-1-4503-9416-1/23/04...\$15.00
<https://doi.org/10.1145/3543507.3583353>

CCS CONCEPTS

• **Information systems** → **Social networks**; **Data mining**; • **Computing methodologies** → **Learning latent representations**; **Neural networks**.

KEYWORDS

Sequential Interaction Network, Graph Neural Network, Dynamics, Riemannian Geometry

ACM Reference Format:

Junda Ye, Zhongbao Zhang, Li Sun, Yang Yan, Feiyang Wang, and Fuxin Ren. 2023. SINCERE: Sequential Interaction Networks representation learning on Co-Evolving Riemannian manifolds. In *Proceedings of the ACM Web Conference 2023 (WWW '23)*, May 1–5, 2023, Austin, TX, USA. ACM, New York, NY, USA, 10 pages. <https://doi.org/10.1145/3543507.3583353>

1 INTRODUCTION

Predicting future interactions for sequential interaction networks is essential in many domains, such as “Guess You Like” in e-commerce recommendation systems [23, 25], “Related Searches” in search engines [4, 24] and “Suggested Posts” in social networks [51, 55]. Specifically, purchasers and commodities form a transaction interaction network recording the trading or rating behaviors on e-commerce platforms, predicting interactions accurately helps improve the quality of item recommendations. Users and posts constitute a social interaction network indicating whether and when a user will click/comment posts, early interventions can be made to prevent teenagers from malicious posts like Internet fraud on social media with the help of interaction prediction.

Graph representation learning plays an important role in demonstrating different nodes in graphs within low-dimensional embeddings. In the literature, the majority of existing studies choose Euclidean space as representation space for its simplicity and efficiency. However, for certain graph topology patterns (e.g., hierarchical, scale-free or spherical data), Euclidean space may suffer from large distortion [9]. Recently, non-Euclidean spaces have emerged as an alternative for their strong capability to embed hierarchical or cyclical data into a low-dimensional space while preserving the structure [21, 31, 57]. Specifically, hyperbolic geometry was first introduced to graph representation learning [18, 34, 35], and

Table 1: The average δ -hyperbolicity [19] of user and item subgraphs on Mooc and Wikipedia dataset along the timeline.

| Dataset | Timeline | User | Item |
|-----------|----------|------|------|
| Mooc | start | 0.77 | 0.50 |
| | middle | 1.0 | 0.67 |
| | end | 1.0 | 0.13 |
| Wikipedia | start | 1.04 | 1.16 |
| | middle | 1.10 | 1.30 |
| | end | 1.33 | 1.40 |

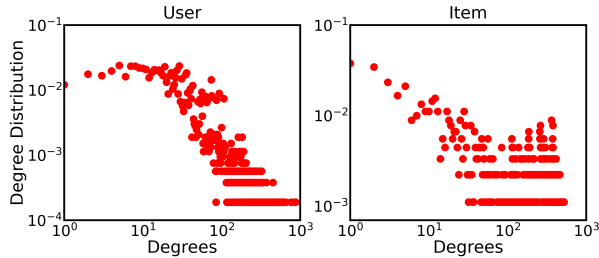


Figure 1: User and item degree distribution on Wikipedia.

then spherical spaces have also gained much attention [13, 37]. The development of representation spaces is prosperous nowadays.

With regard to representing sequential interaction networks, a significant amount of work has been proposed to learn the user and item embeddings from their historical interaction records in Euclidean space [4, 6, 12, 14, 27, 33]. Recurrent models such as Time-LSTM [59], Time-Aware LSTM [3] and RRN [53] capture dynamics of users and items by endowing them with a long short-term memory. HILI [10] is the successor of Jodie [28] and both of them are promising methods for real-world temporal interaction graphs. CTDNE [33] adopts random walk on temporal networks and CAW [51] makes it causal and anonymous to inductively represent sequential networks. Additionally, recent models have been proposed to embed sequential interaction networks into hyperbolic spaces [7, 11, 15, 32, 42]. HyperML [49] investigates the notion of learning user and item representations in terms of metric learning in hyperbolic space. HTGN [55] designs a recurrent architecture on the sequence of snapshots under hyperbolic geometric.

Existing interaction network representation methods did have achieved promising results. However, they still suffer from two major shortcomings. **First**, they simply place *two different* types of nodes (user and item nodes) in *one identical* space, which is ambiguous and counter-intuitive. For instance, viewers and films are two kinds of nodes with totally different characters and distributions which are usually described by the notion of curvature in Riemannian geometry [2, 41, 52]. Here, we give motivated examples in Fig. 1 and Tab. 1 which show that not only the structure of user and item networks varies according to time, but also the degree distribution of users and items are different from each other. Therefore, setting user and item nodes in two spaces seems a proper way and designing an effective message passing mechanism considering cross-space scenarios is challenging. **Second**, they assume the

space is static but in fact the interaction network constantly *evolves* over time, which is mainly ignored in the previous studies. More specifically, they attempt to learn the representations on a single fixed curvature manifold, either Euclidean space or the standard Poincaré Ball. The static curvature is a strong prerequisite that cannot manifest the representation space of inherent dynamics when new edges of the interaction networks are continuously formed. The challenge here is how to estimate the global curvatures accurately for the next period from local structure information. Besides, most of the existing methods [3, 10, 28, 59] also assume that an interaction would only influence corresponding nodes while ignoring the information propagation among the same type of nodes implicitly. New methods are also needed to incorporate the information flow between the same type of nodes.

To overcome the aforementioned shortcomings and challenges, we propose **SINCERE** to represent **S**equential **I**nteraction **N**etworks on **C**o-**E**volving **R**i-**E**mannian manifolds. Specifically, SINCERE sets both user and item nodes in two κ -stereographic spaces, interactions with time embeddings in Euclidean space simultaneously. Next, it estimates the sectional curvatures of two co-evolving spaces according to local structure information through a curvature neural network with shared parameters. Then, the dissemination and integration of information, as well as node embeddings updating are performed through cross-geometry aggregation and updating components in our model. Finally, SINCERE is mainly learned through a Pull-and-Push loss based on maximum likelihood optimization. Extensive experiments validate the performance of SINCERE on several datasets.

The major contributions of this paper are summarized as follows:

- In this paper, we uncover the intrinsic differences between user and item nodes in sequential interaction networks, and model the dynamicity of representation spaces. It is the first attempt to represent sequential interaction networks on a pair of co-evolving Riemannian manifolds to the best we know.
- We propose a novel model SINCERE for sequential interaction networks representation learning. SINCERE represents user and item nodes in dual κ -stereographic spaces with variable curvatures, encoding both immanent dissimilarities and temporal effects of user and item nodes.
- We conduct extensive experiments to evaluate our model with multiple baselines for the tasks of interaction prediction. Experimental results show the superiority and effectiveness of our proposed model.

2 PRELIMINARIES

2.1 Riemannian Manifold

A Riemannian manifold (\mathcal{M}, g) is a real and smooth manifold equipped with an inner product on tangent space $g_{\mathbf{x}} : \mathcal{T}_{\mathbf{x}}\mathcal{M} \times \mathcal{T}_{\mathbf{x}}\mathcal{M} \rightarrow \mathbb{R}$ at each point $\mathbf{x} \in \mathcal{M}$, where the tangent space $\mathcal{T}_{\mathbf{x}}\mathcal{M}$ is the first order approximation of \mathcal{M} around \mathbf{x} , which can be locally seeded Euclidean. The inner product metric tensor $g_{\mathbf{x}}$ is both positive-definite and symmetric, i.e., $g_{\mathbf{x}}(\mathbf{v}, \mathbf{v}) \geq 0$, $g_{\mathbf{x}}(\mathbf{u}, \mathbf{v}) = g_{\mathbf{x}}(\mathbf{v}, \mathbf{u})$ where $\mathbf{x} \in \mathcal{M}$ and $\mathbf{u}, \mathbf{v} \in \mathcal{T}_{\mathbf{x}}\mathcal{M}$.

2.2 The κ -stereographic Model

Hyperboloid and sphere are two common models for hyperbolic and spherical Riemannian geometry. However, hyperbolic space is not a typical vector space, which means we cannot calculate the embedding vectors with operators as if we use in Euclidean space. In order to overcome the gap among hyperbolic, spherical and euclidean geometry, we adopt the κ -stereographic model [2] as it unifies operations with gyrovector formalism [47].

An n -dimension κ -stereographic model is a smooth manifold $\mathcal{M}_\kappa^n = \{\mathbf{x} \in \mathbb{R}^n \mid -\kappa\|\mathbf{x}\|_2^2 < 1\}$ equipped with a Riemannian metric $g_\kappa^\mathbf{x} = (\lambda_\kappa^\mathbf{x})^2 \mathbf{I}$, where $\kappa \in \mathbb{R}$ is the sectional curvature and $\lambda_\kappa^\mathbf{x} = 2(1 + \kappa\|\mathbf{x}\|_2^2)^{-1}$ is the point-wise conformal factor. To be specific, \mathcal{M}_κ^n is the stereographic projection model for spherical space ($\kappa > 0$) and the Poincaré ball model of radius $1/\sqrt{-\kappa}$ for hyperbolic space ($\kappa < 0$), respectively. We first list requisite operators below, specific ones are attached in Appendix. Note that bold letters denote the vectors on the manifold.

Möbius Addition. It is a non-associative addition \oplus_κ of two points $\mathbf{x}, \mathbf{y} \in \mathcal{M}_\kappa^n$ defined as:

$$\mathbf{x} \oplus_\kappa \mathbf{y} = \frac{(1 - 2\kappa\langle \mathbf{x}, \mathbf{y} \rangle - \kappa\|\mathbf{y}\|_2^2) \mathbf{x} + (1 + \kappa\|\mathbf{x}\|_2^2) \mathbf{y}}{1 - 2\kappa\langle \mathbf{x}, \mathbf{y} \rangle + \kappa^2\|\mathbf{x}\|_2^2\|\mathbf{y}\|_2^2}. \quad (1)$$

Möbius Scalar and Matrix Multiplication. The augmented Möbius scalar and matrix multiplication \otimes_κ of $\mathbf{x} \in \mathcal{M}_\kappa^n \setminus \{\mathbf{o}\}$ by $r \in \mathbb{R}$ and $\mathbf{M} \in \mathbb{R}^{m \times n}$ is defined as follows:

$$r \otimes_\kappa \mathbf{x} = \frac{1}{\sqrt{\kappa}} \tanh\left(r \tanh^{-1}(\sqrt{\kappa}\|\mathbf{x}\|_2)\right) \frac{\mathbf{x}}{\|\mathbf{x}\|_2}, \quad (2)$$

$$\mathbf{M} \otimes_\kappa \mathbf{x} = (1/\sqrt{\kappa}) \tanh\left(\frac{\|\mathbf{M}\mathbf{x}\|_2}{\|\mathbf{x}\|_2} \tanh^{-1}(\sqrt{\kappa}\|\mathbf{x}\|_2)\right) \frac{\mathbf{M}\mathbf{x}}{\|\mathbf{M}\mathbf{x}\|_2}. \quad (3)$$

Exponential and Logarithmic Maps. The connection between the manifold \mathcal{M}_κ^n and its point-wise tangent space $\mathcal{T}_\mathbf{x}\mathcal{M}_\kappa^n$ is established by the exponential map $\exp_\kappa^\mathbf{x} : \mathcal{T}_\mathbf{x}\mathcal{M}_\kappa^n \rightarrow \mathcal{M}_\kappa^n$ and logarithmic map $\log_\kappa^\mathbf{x} : \mathcal{M}_\kappa^n \rightarrow \mathcal{T}_\mathbf{x}\mathcal{M}_\kappa^n$ as follows:

$$\exp_\kappa^\mathbf{x}(\mathbf{v}) = \mathbf{x} \oplus_\kappa \left(\tan_\kappa \left(\sqrt{|\kappa|} \frac{\lambda_\kappa^\mathbf{x} \|\mathbf{v}\|_2}{2} \right) \frac{\mathbf{v}}{\|\mathbf{v}\|_2} \right), \quad (4)$$

$$\log_\kappa^\mathbf{x}(\mathbf{y}) = \frac{2}{\lambda_\kappa^\mathbf{x} \sqrt{|\kappa|}} \tan_\kappa^{-1} \left(\frac{-\mathbf{x} \oplus_\kappa \mathbf{y}}{\|-\mathbf{x} \oplus_\kappa \mathbf{y}\|_2} \right). \quad (5)$$

Distance Metric. The generalized distance $d_{\mathcal{M}}^\kappa(\cdot, \cdot)$ between any two points $\mathbf{x}, \mathbf{y} \in \mathcal{M}_\kappa^n$, $\mathbf{x} \neq \mathbf{y}$ is defined as:

$$d_{\mathcal{M}}^\kappa(\mathbf{x}, \mathbf{y}) = \frac{2}{\sqrt{|\kappa|}} \tan_\kappa^{-1} \left(\sqrt{|\kappa|} \|-\mathbf{x} \oplus_\kappa \mathbf{y}\|_2 \right). \quad (6)$$

2.3 Sectional Curvature and Ricci Curvature

In Riemannian geometry, curvature is the amount by which a curve deviates from being a straight line, or a surface deviates from being a plane, which is originally defined on the continuous smooth manifold. Sectional curvature and Ricci curvature are two success formulations for the discrete graph [56], describing the global and local structure, respectively.

Sectional Curvature. Sectional curvature is an equivalent but more geometrical description of the curvature of Riemannian manifolds compared to the Riemann curvature tensor [29]. It is defined over all two-dimensional subspaces passing through a point and

is treated as the constant curvature of a Riemannian manifold in recent work.

Ricci Curvature. Ricci curvature is the average of sectional curvatures and is mathematically a linear operator on tangent space at a point. In graph domain, it is extended to measure how the geometry of a pair of neighbors deviates from the case of grid graphs locally. Ollivier-Ricci [36] is a coarse approach to computing Ricci curvature while Forman-Ricci [16] is combinatorial and faster to compute.

Table 2: Table of symbols used in the paper

| Symbol | Description |
|--------------------------|---------------------------------------|
| \mathcal{U}_{κ_u} | User space with curvature κ_u |
| \mathcal{I}_{κ_i} | Item space with curvature κ_i |
| T_n | Time interval from t_{n-1} to t_n |
| $\kappa_{u/i}^T$ | Curvature of user/item during T |
| $\mathbf{u}(T)$ | Embedding of user u during T |
| $\mathbf{i}(T)$ | Embedding of item i during T |
| $\mathcal{N}_{u/i}^T$ | Neighbors of user/item during T |
| $\mathcal{E}_{u/i}^T$ | Edges linked to user/item during T |

2.4 Problem Definition and Notation

Before presenting our proposed model, we summarize the important notations in Tab. 2. We may drop the subscript indices in later sections for clarity. The definitions of sequential interaction network and representation learning task are stated as follows:

DEFINITION 1 (SEQUENTIAL INTERACTION NETWORK (SIN)). Let $\mathcal{G} = \{\mathcal{U}, \mathcal{I}, \mathcal{E}, \mathcal{T}, \mathcal{X}\}$ denote a sequential interaction network, where \mathcal{U} and \mathcal{I} are two disjoint node sets of user and item, respectively. $\mathcal{E} \subseteq \mathcal{U} \times \mathcal{I} \times \mathcal{T}$ denotes the interaction/edge set, and $\mathcal{X} \in \mathbb{R}^{|\mathcal{E}| \times d_\mathcal{X}}$ is the attributes associated with the interaction. $d_\mathcal{X}$ represents feature dimension. Each edge $e \in \mathcal{E}$ can be indicated as a triplet $e = (u, i, t)$ where $u \in \mathcal{U}$, $i \in \mathcal{I}$, and $t \in \mathcal{T}$ is the timestamp recording that user u and item i interact with each other at time t .

DEFINITION 2 (SIN REPRESENTATION LEARNING TASK). For a sequential interaction network \mathcal{G} , it aims to learn encoding functions $\Phi_u : \mathcal{U} \rightarrow \mathcal{U}_{\kappa_u}$, $\Phi_i : \mathcal{I} \rightarrow \mathcal{I}_{\kappa_i}$ and $\Phi_e : \mathcal{E} \rightarrow \mathbb{E}$ that map two kinds of nodes in networks and interaction between them into dynamic low-dimensional embedding spaces under different Riemannian geometry, where nodes and interaction are represented as compact embedding vectors. Meanwhile, the embeddings capture the intrinsic relation between two types of nodes and are capable of predicting future interactions effectively.

3 SINCERE

Recall that the motivated examples given previously show the intrinsic difference between users and items, to solve the main issues of existing methods on representing sequential interaction networks, we consider the embeddings of user and item residing in different Riemannian manifolds. The two Riemannian manifolds are then bridged by a Euclidean tangent space, which is the representation space of interactions. How the representation spaces evolve over time is told by a curvature estimator.

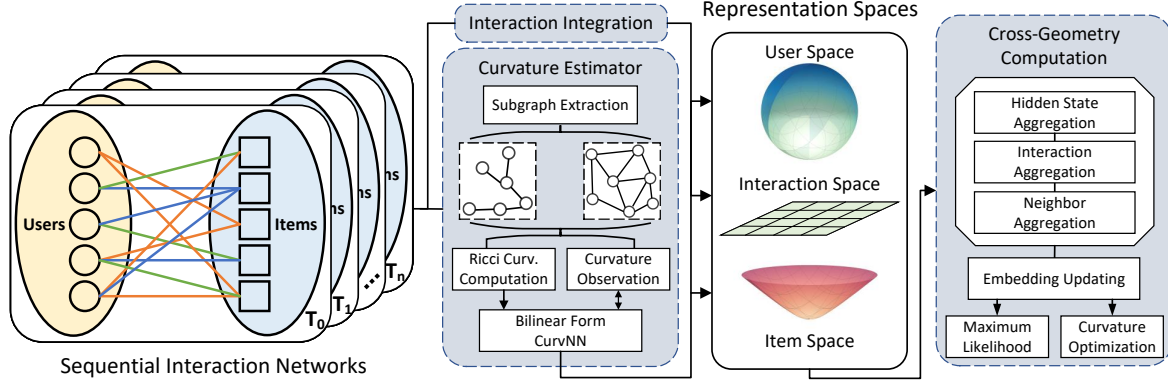


Figure 2: Illustration of SINCERE architecture. We first divide timestamps into several intervals, each of which can be regarded as a batch. Interactions with different colors refer to different timestamps. Next, the graph is sent to the interaction integration component and the curvature estimator for capturing time and structure information, respectively. Then, user and item nodes in different Riemannian manifolds pass neighbor information to each other through novel cross-geometry aggregation and updating. Last, the representation and parameters of SINCERE are optimized through maximum likelihood training objective.

The overall framework of SINCERE is presented in Fig. 2. The components of our approach are introduced in the following.

3.1 User-Item Co-Evolving Mechanism

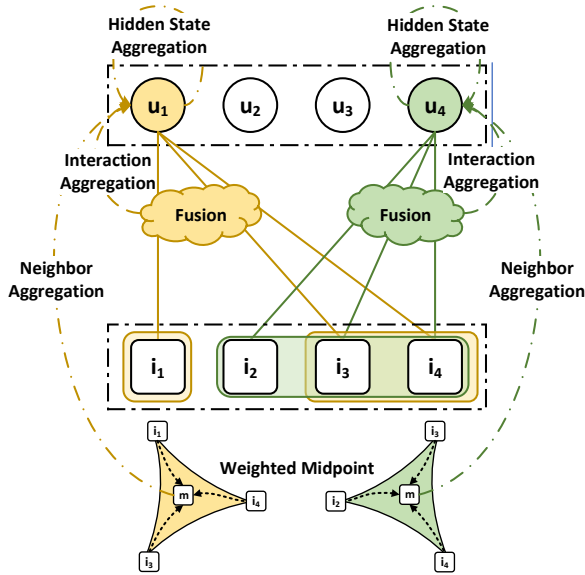


Figure 3: Illustration of one step aggregation. An example of how users update their embeddings from: i) hidden representations, ii) fusion of associated interactions, and iii) weighted midpoint of their neighbors.

As we place the user and item nodes on different Riemannian manifolds, they are recorded by the embedding matrix U and I respectively, which can be initialized with the feature vectors such as the user profiling or film description if available. Since the initialized U and I are in Euclidean space, we logarithmically map them to corresponding Riemannian space \mathbb{U}_{κ_u} and \mathbb{I}_{κ_i} with Eq. (5).

For the message propagation and information aggregation, the design of SINCERE not only incorporates the information across different geometric spaces via a unified formalism, but also guarantees that all operations are conformal invariant. For clarity of expressions, we define map operation to map the vectors in manifold \mathcal{M}_{κ_1} to \mathcal{M}_{κ_2} as $\text{map}_{\kappa_1}^{\kappa_2}(\cdot) := \exp_{\mathbf{o}}^{\kappa_2}(\log_{\mathbf{o}}^{\kappa_1}(\cdot))$. The aggregation operators of user and item are defined as follows:

$$\mathbf{u}_j(T_n) \leftarrow \underbrace{\mathbf{M}_1 \otimes_{\kappa_u^T} \mathbf{h}_{u_j}(T_n)}_{\text{user hidden aggregation}} \oplus_{\kappa_u^T} \underbrace{\mathbf{M}_2 \otimes_{\kappa_u^T} \exp_{\mathbf{o}}^{\kappa_u^T}(\mathbf{e}'_{u_j^T})}_{\text{interaction aggregation}} \oplus_{\kappa_u^T} \underbrace{\mathbf{M}_3 \otimes_{\kappa_u^T} \text{map}_{\kappa_i^T}^{\kappa_u^T}(\mathbf{i}'_{u_j^T})}_{\text{item aggregation}}, \quad (7)$$

$$\mathbf{i}_k(T_n) \leftarrow \underbrace{\mathbf{M}_4 \otimes_{\kappa_i^T} \mathbf{h}_{i_k}(T_n)}_{\text{item hidden aggregation}} \oplus_{\kappa_i^T} \underbrace{\mathbf{M}_5 \otimes_{\kappa_i^T} \exp_{\mathbf{o}}^{\kappa_i^T}(\mathbf{e}'_{i_k^T})}_{\text{interaction aggregation}} \oplus_{\kappa_i^T} \underbrace{\mathbf{M}_6 \otimes_{\kappa_i^T} \text{map}_{\kappa_u^T}^{\kappa_i^T}(\mathbf{u}'_{i_k^T})}_{\text{user aggregation}}, \quad (8)$$

where \mathbf{M} s are trainable matrices and \mathbf{h} represents hidden state. The aggregation operator has three main components: hidden state aggregation, interaction aggregation and neighbor aggregation.

Take the user aggregation shown in Eq. (7) and Fig. 3 as an example: the first component is the update of user j hidden representation for several layers, which can be cascaded for multi-hop message aggregation, and the second component aggregates the associated edge information to user j and the third component aggregates items information which is interacted by user j . *It is worth noting that the problem of ignoring the information propagation among the same type of nodes can be solved by stacking several layers.* $e'_{u/i}$ in the interaction aggregation is either *Early Fusion* $e'_{u/i} = \text{MLP}(\text{POOLING}(\mathbf{e} \in \mathcal{E}_{u/i}^T))$ or *Late Fusion* $e'_{u/i} = \text{POOLING}(\text{MLP}(\mathbf{e} \in \mathcal{E}_{u/i}^T))$ and $\text{POOLING}(\cdot)$ can be one of the Mean Pooling and Max Pooling. \mathbf{i}'_u and \mathbf{u}'_i in neighbor aggregation are the **weighted gyro-midpoints** [48] (specified in the Appendix) in item and user stereographic spaces, respectively. Take \mathbf{i}'_u as an example, which is defined as:

$$\mathbf{i}'_u = \text{MIDPOINT}_{\kappa_i^T}(\mathbf{x}_j \in \mathcal{N}_u^T) = \frac{1}{2} \otimes_{\kappa_i^T} \left(\sum_{\mathbf{x}_j \in \mathcal{N}_u^T} \frac{\alpha_k \lambda_{\mathbf{x}_j}^\kappa}{\sum_{\mathbf{x}_k \in \mathcal{N}_u^T} \alpha_k (\lambda_{\mathbf{x}_k}^\kappa - 1)} \mathbf{x}_j \right), \quad (9)$$

where α_k is attention weight and $\lambda_{\mathbf{x}}^\kappa$ is point-wise conformal factor.

After the aggregation of nodes and edges, we project embeddings to next-period manifolds for further training and predicting. The node updating equation is defined as follows:

$$\mathbf{u}_j(T_{n+1}) = \text{map}_{\kappa_u^{T_{n+1}}}^{\kappa_u^{T_n}}(\mathbf{u}_j(T_n)), \quad (10)$$

$$\mathbf{i}_j(T_{n+1}) = \text{map}_{\kappa_i^{T_{n+1}}}^{\kappa_i^{T_n}}(\mathbf{i}_j(T_n)), \quad (11)$$

where the curvature $\kappa^{T_{n+1}}$ of next interval can be obtained from Eq. (16).

3.2 Interaction Modeling

We set the sequential interactions in Euclidean space instead of on Riemannian manifolds as user and item nodes. The intuition behind such design is that the tangent space which is Euclidean is the common space of different Riemannian manifolds and users and items are linked by sequential interactions. Specifically, for an edge $e_k \in \mathcal{E}$, the integration of its corresponding attribute $\mathbf{X}_k \in \mathcal{X}$ and timestamp $t_k \in \mathcal{T}$ is regarded as the initialized embedding. In order to capture the temporal information of interactions, we formalize the time encoder as a function $\Phi_t: \mathbb{R} \rightarrow \mathbb{R}^d$ which maps a continuous time t_k to a d -dimensional vector. In order to account for time translation invariance in consideration of the aforementioned batch setup, we adopt the *harmonic encoder* [54] as follows:

$$\phi(t) = \sqrt{\frac{1}{d}} [\cos(\omega_1 t + \theta_1); \cos(\omega_2 t + \theta_2); \dots; \cos(\omega_d t + \theta_d)], \quad (12)$$

where ω s and θ s are learnable encoder parameters. and $[\cdot; \cdot]$ is the concatenation operator. *The definition of Eq. (12) satisfies time translation invariance.* Thus, the initial embedding of the interaction e_k can be represented as:

$$\mathbf{e}_k = \sigma(\mathbf{W}_1 \cdot [\mathbf{X}_k; \phi(t_k)]), \quad (13)$$

where $\sigma(\cdot)$ is the activation function and \mathbf{W}_1 is the training matrix.

3.3 Curvature Estimator

Embedding vectors of the previous work are set on one fixed curvature manifold such as Poincaré Ball, while the fixed curvature is a strong premise assumption which cannot manifest the dynamics of the representation space. In fact, the curvature of the embedding space evolves over time, and thus we need to design curvature computation for both local curvature and global curvature, *i.e.*, Ricci curvature and sectional curvature.

Sequential interaction networks are mostly bipartite graphs, which means there is no direct link connected between nodes of the same type. Therefore, to explore the local Ricci curvature in both user and item spaces, we need to extract new topologies from the input network. The rule of subgraph extraction is based on the shared neighbor relationship, *e.g.*, users with common item neighbors are friends with each other. However, there will be several complete graphs which increase the complexity if we let all users with the same neighbors become friends. Here, we take sampling in extracting subgraph process to avoid long time cost. Then, the local curvature of any edge (x, y) can be resolved by Ollivier-Ricci curvature κ_r defined as follows:

$$\kappa_r(x, y) = 1 - \frac{W(m_x, m_y)}{d_{\mathcal{M}}^\kappa(x, y)}, \quad (14)$$

where $W(\cdot, \cdot)$ is Wasserstein distance (or Earth Mover distance) which finds the optimal mass-preserving transportation plan between two probability measures. m_x is the mass distribution of the node x measuring the importance distribution of one node among its one-hop neighbors $\mathcal{N}(x) = \{x_1, x_2, \dots, x_l\}$, which is defined as:

$$m_x^\alpha(x_i) = \begin{cases} \alpha & \text{if } x_i = x, \\ (1 - \alpha)/l & \text{if } x_i \in \mathcal{N}(x), \\ 0 & \text{otherwise.} \end{cases} \quad (15)$$

where α is a hyper-parameter within $[0, 1]$. Similar to previous work [38, 56], we set $\alpha = 0.5$.

Algorithm 1: Curvature Observation

Input : An undirected graph G , iterations n

Output: Observed curvature κ_o

```

1 for  $m \in G$  do
2   for  $i = 1, \dots, n$  do
3      $b, c \in \text{Sample}(\mathcal{N}(m))$  and  $a \in \text{Sample}(G) \setminus \{m\}$ ;
4     Calculate  $\gamma_{\mathcal{M}}(a, b, c)$ ;
5     Calculate  $\gamma_{\mathcal{M}}(m; b, c, a)$ ;
6   Let  $\gamma(m) = \text{MEAN}(\gamma_{\mathcal{M}}(m; b, c, a))$ ;
7 Return:  $\kappa_o = \text{MEAN}(\gamma(m))$ 

```

Let \mathbf{R} represent the vector of Ricci curvatures. Inspired by the bilinear form between Ricci curvature and sectional curvature, we design the global sectional curvature neural network called *CurvNN* as follows:

$$\kappa_e = \text{MLP}(\mathbf{R})^T \mathbf{W}_2 \text{MLP}(\mathbf{R}), \quad (16)$$

where W_2 is the trainable matrix and MLP means multilayer perceptron. The bilinear design of *CurvNN* allows us to obtain the sectional curvature of any sign.

The observation of the curvature is also important for us to train *CurvNN*. Therefore, we adopt a variant of the Parallelogram Law to observe the sectional curvature [2, 17, 20]. Considering a geodesic triangle abc on manifold \mathcal{M} and m is the midpoint of bc , two of their quantities are defined as: $\gamma_{\mathcal{M}}(a, b, c) := d_{\mathcal{M}}(a, m)^2 + d_{\mathcal{M}}(b, c)^2 / 4 - (d_{\mathcal{M}}(a, b)^2 + d_{\mathcal{M}}(a, c)^2) / 2$ and $\gamma_{\mathcal{M}}(m; b, c; a) := \frac{\gamma_{\mathcal{M}}(a, b, c)}{2d_{\mathcal{M}}(a, m)}$. The observed curvature is calculated in Algorithm 1. The observed curvature κ_o will supervise the training of *CurvNN* to generate estimated curvature κ_e accurately as possible.

3.4 Training Objective

Benefiting from the fact that the output of SINCERE is embedded representation of users and items, we can treat them as input to various downstream tasks, such as interaction prediction. If we easily add up the distance from different spaces, the distortion will be huge due to different geometry metrics. Therefore, we consider our optimization from two symmetric aspects, *i.e.*, user and item. Specifically, we first map the item embedding to user space and calculate the distance under user geometry metric, and vice versa as follows:

$$\begin{aligned} d_{\mathcal{U}}(\mathbf{u}, \mathbf{i}) &= d_{\kappa_u}(\mathbf{u}, \text{map}_{\kappa_i}^{\kappa_u}(\mathbf{i})), \\ d_{\mathcal{I}}(\mathbf{u}, \mathbf{i}) &= d_{\kappa_i}(\text{map}_{\kappa_u}^{\kappa_i}(\mathbf{u}), \mathbf{i}). \end{aligned} \quad (17)$$

Then, we regard Fermi-Dirac decoder, a generalization of Sigmoid, as the likelihood function to compute the connection probability between users and items in both spaces. Since we convert the distance into probabilities, the probabilities then can be easily summed. Moreover, we are curious about which geometric manifolds are more critical for interaction prediction, and then assign more weight to the corresponding probability. The likelihood function and probability assembling are defined as follows:

$$P_{\mathcal{U}/\mathcal{I}}(e|\Theta) = \frac{1}{\exp\left(\left(d_{\mathcal{U}/\mathcal{I}}(\mathbf{u}, \mathbf{i}) - r\right)/t\right) + 1}, \quad (18)$$

$$P(e|\Theta) = \rho P_{\mathcal{U}} + (1 - \rho)P_{\mathcal{I}}, \quad (19)$$

where Θ represents all learnable parameters in SINCERE, $r, t > 0$ are hyperparameters of Fermi-Dirac decoder, and ρ is the learnable weight. Users and items share the same formulation of the likelihood.

The main optimization is based on the idea of Pull-and-Push. We hope that the embedding in batch T_n is capable of predicting the interaction in batch T_{n+1} , thus we utilize the graph in batch T_{n+1} to supervise the previous batch. In particular, we expect a greater probability for all interactions that actually occur in next batch, but a smaller probability for all the negative samples. Given the large number of negative samples, we determine to use negative sampling (Gaussian) with rate of 20% and it can also avoid the problem of over-fitting. For the curvature estimator component, we wish that *CurvNN* can learn the global sectional curvature from the local structure (Ricci curvature) without observing in the prediction task. Therefore, we make the Euclidean norm of estimated curvature κ_e and observed curvature κ_o as our optimizing target. We calculate

the total loss as follows:

$$\begin{aligned} \Theta^* &= \underset{\Theta}{\operatorname{argmax}} \sum_{e \in \mathcal{E}} \ln[P(e|\Theta)] \\ &\quad - \text{Sampling} \left(\sum_{e \notin \mathcal{E}} \ln[P(e|\Theta)] \right) + \|\kappa_e - \kappa_o\|_2. \end{aligned} \quad (20)$$

3.5 Computational Complexity Analysis

The procedure of training SINCERE is given in appendix. The curvature estimator and cross-geometry operations are two main processes of SINCERE. To avoid excessive parameters, we use a shared curvature estimator for both user and item spaces. The primary computational complexity of SINCERE is approximated as $O(|\mathcal{U}|DD' + |\mathcal{I}|DD' + |\mathcal{E}|D'^2) + O(V^3 \log V)$, where $|\mathcal{U}|$ and $|\mathcal{I}|$ are number of user and item nodes and $|\mathcal{E}|$ is the number of interactions. D and D' are the dimensions of input and hidden features respectively and V is the total number of vertices in the Wasserstein distance sub-problem. The former $O(\cdot)$ is the computational complexity of all aggregating and updating operations and the computation of other parts in our model can be parallelized and is computationally efficient. The latter $O(\cdot)$ is the complexity of Olliver-Ricci curvature. In order to avoid repeated calculation of Ricci curvature, we adopt an **OFFLINE** pre-computation that calculates Ricci curvatures according to different batch sizes and saves it in advance since the subgraph in each batch does not change.

4 EXPERIMENTS

4.1 Datasets and Compared Algorithms

Datasets. We conduct experiments on five dynamic real-world datasets: **MOOC**, **Wikipedia**, **Reddit**, **LastFM** and **Movielens** to evaluate the effectiveness of SINCERE. The description and statistic details of these datasets are shown in Appendix.

Compared Algorithms. To demonstrate the effectiveness of our method, we compare our model with nine state-of-the-art models, categorized as follows:

- **Recurrent sequence models:** we compare with different flavors of RNNs trained for item-sequence data: LSTM, TimeLSTM [59], RRN [53].
- **Random walk based models:** CAW [51], CTDNE [33] are two temporal network models adopting causal and anonymous random walks.
- **Sequence network embedding models:** in this category, JODIE [28], HILI [10] and DeepRed [27] are three state-of-the-art methods in generating embeddings from sequential networks employing recursive networks.
- **Hyperbolic models:** we compare SINCERE with HGCF [42] which is a hyperbolic method on collaborative filtering.

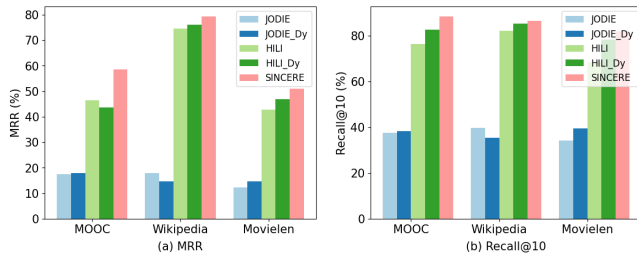
4.2 Future Interaction Prediction

The goal of the future interaction prediction task is to predict the next item a user is likely to interact with based on observations of recent interactions. We here use two metrics, mean reciprocal rank (MRR) and Recall@10 to measure the performance of all methods. The higher the metrics, the better the performance. For fair comparison, all models are run for 50 epochs and the dimension

Table 3: Future interaction prediction: Performance comparison in terms of mean reciprocal rank (MRR) and Recall@10. The best results are in bold and second best results are underlined.

| Datasets → Methods ↓ | MOOC | | Wikipedia | | Reddit | | LastFM | | Movielen | |
|-------------------------|--------------|--------------|--------------|--------------|--------------|--------------|--------------|--------------|--------------|--------------|
| | MRR | Recall@10 |
| LSTM | 0.055 | 0.109 | 0.329 | 0.455 | 0.355 | 0.551 | 0.062 | 0.119 | 0.031 | 0.060 |
| Time-LSTM [59] | 0.079 | 0.161 | 0.247 | 0.342 | 0.387 | 0.573 | 0.068 | 0.137 | 0.046 | 0.084 |
| RRN [53] | 0.127 | 0.230 | 0.522 | 0.617 | 0.603 | 0.747 | 0.089 | 0.182 | 0.072 | 0.181 |
| CAW [51] | 0.200 | 0.427 | 0.656 | 0.862 | 0.672 | 0.794 | 0.121 | 0.272 | 0.096 | 0.243 |
| CTDNE [33] | 0.173 | 0.368 | 0.035 | 0.056 | 0.165 | 0.257 | 0.01 | 0.01 | 0.033 | 0.051 |
| JODIE [28] | <u>0.465</u> | 0.765 | 0.746 | 0.822 | 0.726 | 0.852 | 0.195 | 0.307 | 0.428 | 0.685 |
| HILI [10] | 0.436 | <u>0.826</u> | 0.761 | 0.853 | 0.735 | 0.868 | 0.252 | <u>0.427</u> | <u>0.469</u> | <u>0.784</u> |
| DeePRed [27] | 0.458 | 0.532 | 0.885 | 0.889 | 0.828 | <u>0.833</u> | <u>0.393</u> | 0.416 | 0.441 | 0.472 |
| HGCF [42] | 0.284 | 0.618 | 0.123 | 0.344 | 0.239 | 0.483 | 0.040 | 0.083 | 0.108 | 0.260 |
| SINCERE (ours) | 0.586 | 0.885 | <u>0.793</u> | <u>0.865</u> | <u>0.825</u> | 0.883 | 0.425 | 0.466 | 0.511 | 0.819 |

of embeddings for most models are set to 128. We use a chronological train-valid-test split with a ratio of 80%-10%-10% following other baselines. We use the validation set to tune SINCERE hyperparameters using Adam optimization with a learning rate of 3×10^{-3} .

**Figure 4: Comparison between methods and the ones without static embeddings on future interaction prediction.**

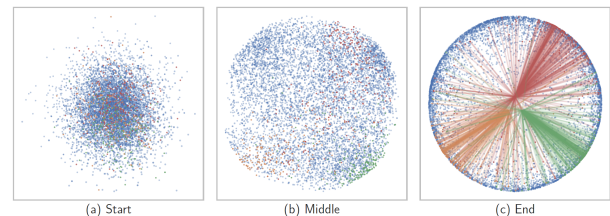
During testing, given a former period of interactions, SINCERE first estimates the sectional curvature of the next period based on the structure information, then calculates the link probability between the specific user and all items and predicts a ranked top- k items list. The experimental results are reported in Tab. 3, where all the baselines use the parameters of the best performance according to the original papers. In general, our method performs the best against other methods, demonstrating the benefits of dual spaces design and representation spaces dynamics. Among all methods, we find that SINCERE and DeePRed have the smallest gaps between MRR and Recall@10, which means not only can these two models find the exact items the user may interact with, but also can distinguish the ground truth from negative samples with higher ranks.

While predicting future interactions, we discover that the performance of two state-of-the-art methods JODIE and HILI have little vibration with the embedding size from 32 to 256 compared with other methods, which means they are insensitive to the embedding size. We argue that the robustness to embedding size is actually

irrelevant to the merit of the model itself and we argue that JODIE and HILI have a relatively strong reliance on static embeddings which are one-hot vectors. To verify this, we have further investigation on the results of removing static embeddings (one-hot vectors). In Fig. 4, JODIE_Dy and HILI_Dy indicates the ones with no static embedding. JODIEs are in blue schemes and HILIs in green. The experimental result shows that there is a huge gap once the one-hot vectors are removed which verifies our assumption, while SINCERE performs the best in terms of MRR and Recall@10. Besides, HILI relies less on the static embeddings for the greater gain between HILI and HILI_Dy compared to JODIE.

4.3 Ablation Analysis

The introduction of co-evolving κ -stereographic spaces is the basis of SINCERE. In order to analyze the effect of dynamic modeling and co-evolving κ -stereographic spaces, we conduct ablation experiments on four datasets with two variant models named SINCERE-Static and SINCERE- \mathbb{E} , respectively.

**Figure 5: A visualization of three different status of SINCERE-Static on Movielen dataset. We follow and color the movie nodes viewed by three users in red, orange and green. Others are in blue. Central convergence points are the three users we pick and map from user space.**

For SINCERE-Static, we setup the static curvature from the training beginning the same as last-batch curvature of the previous experiment to make the spaces steady. For SINCERE- \mathbb{E} , we fix the curvature to zero as the space is Euclidean. As shown in Tab. 4, the

Table 4: Comparison on different variants of SINCERE.

| Datasets → Methods ↓ | MOOC | | Wikipedia | | Reddit | | Movielen | |
|-------------------------|--------------|--------------|--------------|--------------|--------------|--------------|--------------|--------------|
| | MRR | Recall@10 | MRR | Recall@10 | MRR | Recall@10 | MRR | Recall@10 |
| SINCERE | 0.586 | 0.885 | 0.793 | 0.865 | 0.825 | 0.883 | 0.511 | 0.819 |
| SINCERE-Static | 0.469 | 0.813 | 0.747 | 0.834 | 0.703 | 0.775 | 0.402 | 0.664 |
| SINCERE- \mathbb{E} | 0.397 | 0.674 | 0.692 | 0.758 | 0.682 | 0.723 | 0.374 | 0.616 |

performance of SINCERE-Static is closer to SINCERE compared with SINCERE- \mathbb{E} which is because the curvature set in SINCERE-Static can be seen as the pseudo-optimal curvature. The small gap indicates that there is some information loss in the training process even though the pseudo-optimal curvature is given. Fig. 5 gives an visualization of SINCERE-Static on Movielen dataset with curvature set to -1 . The performance of fixing the space as Euclidean is somehow less competitive, which confirms that introducing dual dynamic Riemannian manifolds is necessary and effective.

4.4 Hyperparameter Sensitivity Analysis

To further investigate the performance of SINCERE, we conduct several experiments for SINCERE with different setups to analyze its sensitivity to hyperparameters.

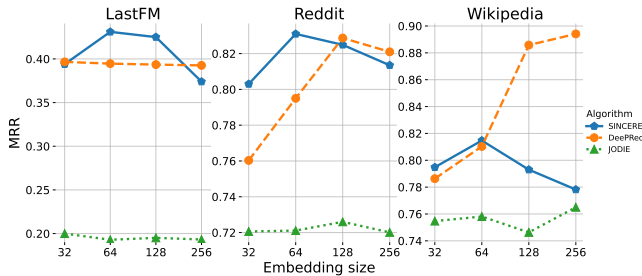
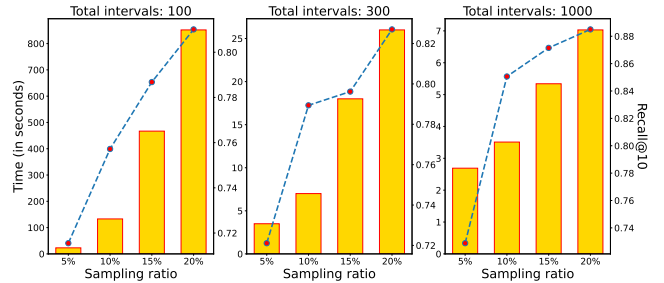
**Figure 6: Effect of embedding size.**

Fig. 6 shows the impact of embedding dimension on the performance of three methods. 128 seems an optimal value for DeepRED in most cases. As we discuss in Sec. 4.2, JODIE counts on the static embeddings which makes embedding size have almost no influence on it. However, we find that in some cases such as LastFM and Wikipedia, SINCERE performs better with dimension 64 than 128 and we argue that it is due to the strong representational power of hyperbolic spaces. In these cases, 64 is capable enough to represent the networks.

The time spent in computing Ricci curvatures and the influence of subgraph extraction sampling ratio on SINCERE performance are shown in Fig. 7. We observe that the computing time decreases sharply with the number of total intervals increase. Besides, the performance (Recall@10) levels off from the sampling ratio 15% to 20% as interval number grows. Such finding informs us that instead of increasing sampling rate to improve performance, it is far better to set a higher interval number considering the computational complexity of Ricci curvatures.

**Figure 7: Effect of sample ratio on MOOC dataset.**

5 RELATED WORK

Sequential Graph Representation. Graph representation assigns individual node an embedding integrating structure and attribute information. Sequential interaction graph representation takes temporal dependency into consideration [1, 26], and temporal graph neural networks achieve great success recently [22, 44, 50, 54, 60]. Among them, RNN based models [3, 4, 53, 59] are the most popular due to effectiveness on sequential data. CTDNE [33] and CAW [51] adopt random walk to temporal graph modeling. Co-evolution models consider the influence between users and items and achieve great success [10, 12, 27, 28]. For systematic and comprehensive reviews, readers may refer to [1, 26].

Riemannian Graph Learning. Hyperbolic and spherical manifolds are typical instances of Riemannian manifolds and recently serve as the alternative of Euclidean spaces, solving distortion problems. A series of Riemannian graph models are proposed [5, 8, 30, 40, 43, 46]. Recently, to match the wide variety of graph structures, the study of mixed-curvature space has been conducted. For instance, MVAE [39] and SelfMGNN [45] are two recent representatives to capture the complex graph structure in product manifolds. As another line of work, GIL [58] attempts to embed a graph into the Euclidean space and hyperbolic space simultaneously for interaction learning.

6 CONCLUSION

In this paper, we take the first attempt to study the sequential interaction network representation learning in co-evolving Riemannian spaces, and present a novel model SINCERE. Specifically, we first introduce a couple of co-evolving Riemannian representation spaces for both types of nodes bridged by the Euclidean-like tangent space. Then, we design the sectional curvature estimator and geometry-cross methods for space evolution trend prediction and message propagation. Finally, we conduct extensive experiments on several real-world datasets and show the superiority of SINCERE.

ACKNOWLEDGMENTS

This work was supported in part by National Natural Science Foundation of China under Grant U1936103, 61921003 and 62202164.

REFERENCES

- [1] Charu Aggarwal and Karthik Subbian. 2014. Evolutionary Network Analysis: A Survey. *ACM Computing Surveys (CSUR)* 47, 1 (2014), 1–36.
- [2] Gregor Bachmann, Gary Becigneul, and Octavian Ganea. 2020. Constant Curvature Graph Convolutional Networks. In *Proceedings of the 37th International Conference on Machine Learning (Proceedings of Machine Learning Research, Vol. 119)*, Hal Daumé III and Aarti Singh (Eds.). PMLR, 486–496. <https://proceedings.mlr.press/v119/bachmann20a.html>
- [3] Inci M Baytas, Cao Xiao, Xi Zhang, Fei Wang, Anil K Jain, and Jiayu Zhou. 2017. Patient Subtyping via Time-aware LSTM Networks. In *Proceedings of the 23rd ACM SIGKDD International Conference on Knowledge Discovery and Data Mining*, 65–74.
- [4] Alex Beutel, Paul Covington, Sagar Jain, Can Xu, Jia Li, Vince Gatto, and Ed H. Chi. 2018. Latent Cross: Making Use of Context in Recurrent Recommender Systems. In *Proceedings of the Eleventh ACM International Conference on Web Search and Data Mining (Marina Del Rey, CA, USA) (WSDM '18)*. Association for Computing Machinery, New York, NY, USA, 46–54. <https://doi.org/10.1145/3159652.3159727>
- [5] Johann Brehmer and Kyle Cranmer. 2020. Flows for Simultaneous Manifold Learning and Density Estimation. In *Advances in Neural Information Processing Systems*, H. Larochelle, M. Ranzato, R. Hadsell, M.F. Balcan, and H. Lin (Eds.), Vol. 33. Curran Associates, Inc., 442–453. <https://proceedings.neurips.cc/paper/2020/file/051928341be67dcb03f0e04104d9047-Paper.pdf>
- [6] Jiangxia Cao, Xixun Lin, Shu Guo, Luchen Liu, Tingwen Liu, and Bin Wang. 2021. Bipartite Graph Embedding via Mutual Information Maximization. In *Proceedings of the 14th ACM International Conference on Web Search and Data Mining*, 635–643.
- [7] Benjamin Paul Chamberlain, Stephen R Hardwick, David R Wardrop, Fabon Dzongang, Fabio Daolio, and Saúl Vargas. 2019. Scalable Hyperbolic Recommender Systems. *arXiv preprint arXiv:1902.08648* (2019). <https://arxiv.org/pdf/1902.08648.pdf>
- [8] Ines Chami, Albert Gu, Vaggos Chatziafatis, and Christopher Ré. 2020. From Trees to Continuous Embeddings and Back: Hyperbolic Hierarchical Clustering. In *Advances in Neural Information Processing Systems*, H. Larochelle, M. Ranzato, R. Hadsell, M.F. Balcan, and H. Lin (Eds.), Vol. 33. Curran Associates, Inc., 15065–15076. <https://proceedings.neurips.cc/paper/2020/file/ac10ec1ace51b2d973cd87973a98d3ab-Paper.pdf>
- [9] Ines Chami, Zhitao Ying, Christopher Ré, and Jure Leskovec. 2019. Hyperbolic Graph Convolutional Neural Networks. *Advances in Neural Information Processing Systems* 32 (2019).
- [10] Huidi Chen, Yun Xiong, Yangyong Zhu, and Philip S. Yu. 2021. Highly Liquid Temporal Interaction Graph Embeddings. In *Proceedings of the Web Conference 2021 (Ljubljana, Slovenia) (WWW '21)*. Association for Computing Machinery, New York, NY, USA, 1639–1648. <https://doi.org/10.1145/3442381.3449921>
- [11] Jacek Dąbrowski, Barbara Rychalska, Michał Daniluk, Dominika Basaj, Konrad Goluchowski, Piotr Babel, Andrzej Michalowski, and Adam Jakubowski. 2021. An Efficient Manifold Density Estimator for All Recommendation Systems. In *Neural Information Processing: 28th International Conference, ICONIP 2021, Sanur, Bali, Indonesia, December 8–12, 2021, Proceedings, Part IV 28*. Springer, 323–337.
- [12] Hanjun Dai, Yichen Wang, Rakshit Trivedi, and Le Song. 2016. Deep Coevolutionary Network: Embedding User and Item Features for Recommendation. *arXiv preprint arXiv:1609.03675* (2016). <https://arxiv.org/pdf/1609.03675.pdf>
- [13] Michaël Defferrard, Martino Milani, Frédéric Gusset, and Nathanaël Perraudin. 2020. DeepSphere: a Graph-based Spherical CNN. In *International Conference on Learning Representations*. <https://openreview.net/forum?id=B1e3OlStPB>
- [14] Ziwei Fan, Zhiwei Liu, Jiawei Zhang, Yun Xiong, Lei Zheng, and Philip S Yu. 2021. Continuous-time Sequential Recommendation with Temporal Graph Collaborative Transformer. In *Proceedings of the 30th ACM International Conference on Information & Knowledge Management*, 433–442.
- [15] Shanshan Feng, Lucas Vinh Tran, Gao Cong, Lisi Chen, Jing Li, and Fan Li. 2020. Hme: A Hyperbolic Metric Embedding Approach for Next-poi Recommendation. In *Proceedings of the 43rd International ACM SIGIR Conference on Research and Development in Information Retrieval*, 1429–1438.
- [16] Robin Forman. 2003. Bochner's Method for Cell Complexes and Combinatorial Ricci Curvature. *Discrete and Computational Geometry* 29, 3 (2003), 323–374.
- [17] Xingcheng Fu, Jianxin Li, Jia Wu, Qingyun Sun, Cheng Ji, Senzhang Wang, Jiajun Tan, Hao Peng, and Philip S. Yu. 2021. ACE-HGNN: Adaptive Curvature Exploration Hyperbolic Graph Neural Network. In *2021 IEEE International Conference on Data Mining (ICDM)*. IEEE, 111–120.
- [18] Octavian Ganea, Gary Becigneul, and Thomas Hofmann. 2018. Hyperbolic Neural Networks. In *Advances in Neural Information Processing Systems*, 5345–5355.
- [19] M. Gromov. 1987. *Hyperbolic Groups*. Springer New York, New York, NY, 75–263. https://doi.org/10.1007/978-1-4613-9586-7_3
- [20] Albert Gu, Frederic Sala, Beliz Gunel, and Christopher Ré. 2019. Learning Mixed-Curvature Representations in Product Spaces. In *International Conference on Learning Representations*. <https://openreview.net/forum?id=HJxeWnCcF7>
- [21] Caglar Gulcehre, Misha Denil, Mateusz Malinowski, Ali Razavi, Razvan Pascanu, Karl Moritz Hermann, Peter Battaglia, Victor Bapst, David Raposo, Adam Santoro, and Nando de Freitas. 2019. Hyperbolic Attention Networks. In *International Conference on Learning Representations*.
- [22] Shubham Gupta, Sahil Manchanda, Srikanta Bedathur, and Sayan Ranu. 2022. TIGGER: Scalable Generative Modelling for Temporal Interaction Graphs. In *Proceedings of the AAAI Conference on Artificial Intelligence*, Vol. 36, 6819–6828.
- [23] Xiangnan He, Ming Gao, Min-Yen Kan, Yiqun Liu, and Kazunari Sugiyama. 2014. Predicting the Popularity of Web 2.0 Items Based on User Comments. In *Proceedings of the 37th International ACM SIGIR Conference on Research and Development in Information Retrieval*, 233–242.
- [24] Zhipeng Huang, Bogdan Cautis, Reynold Cheng, Yudian Zheng, Nikos Mamoulis, and Jing Yan. 2018. Entity-Based Query Recommendation for Long-Tail Queries. *ACM Trans. Knowl. Discov. Data* 12, 6, Article 64 (aug 2018), 24 pages. <https://doi.org/10.1145/3233186>
- [25] Shan Jiang, Yuening Hu, Changsung Kang, Tim Daly Jr, Dawei Yin, Yi Chang, and Chengxiang Zhai. 2016. Learning Query and Document Relevance from a Web-scale Click Graph. In *Proceedings of the 39th International ACM SIGIR Conference on Research and Development in Information Retrieval*, 185–194.
- [26] Seyed Mehran Kazemi, Rishab Goel, Kshitij Jain, Ivan Kobyzev, Akshay Sethi, Peter Forsyth, and Pascal Poupard. 2020. Representation Learning for Dynamic Graphs: A Survey. *Journal of Machine Learning Research* 21, 70 (2020), 1–73.
- [27] Zekarias Kefato, Sarunas Girdzijauskas, Nasrullah Sheikh, and Alberto Montresor. 2021. Dynamic Embeddings for Interaction Prediction. In *Proceedings of the Web Conference 2021*, 1609–1618.
- [28] Srijan Kumar, Xikun Zhang, and Jure Leskovec. 2019. Predicting Dynamic Embedding Trajectory in Temporal Interaction Networks. In *Proceedings of the 25th ACM SIGKDD International Conference on Knowledge Discovery & Data Mining*, 1269–1278.
- [29] John M Lee. 2018. *Introduction to Riemannian Manifolds*. Springer.
- [30] Qi Liu, Maximilian Nickel, and Douwe Kiela. 2019. Hyperbolic Graph Neural Networks. In *Advances in Neural Information Processing Systems*, H. Wallach, H. Larochelle, A. Beygelzimer, F. d'Alché-Buc, E. Fox, and R. Garnett (Eds.), Vol. 32. Curran Associates, Inc. <https://proceedings.neurips.cc/paper/2019/file/103303dd56a731e377d01f6a37badae3-Paper.pdf>
- [31] Emile Mathieu, Charline Le Lan, Chris J Maddison, Ryota Tomioka, and Yee Whye Teh. 2019. Continuous Hierarchical Representations with Poincaré Variational Auto-Encoders. In *Advances in Neural Information Processing Systems*, 12544–12555.
- [32] Leyla Mirvakhabova, Evgeny Frolov, Valentin Khruikov, Ivan Oseledets, and Alexander Tuzhilin. 2020. Performance of Hyperbolic Geometry Models on Top-N Recommendation Tasks. In *Proceedings of the 14th ACM Conference on Recommender Systems*, 527–532.
- [33] Giang Hoang Nguyen, John Boaz Lee, Ryan A Rossi, Nesreen K Ahmed, Eunyee Koh, and Sunghul Kim. 2018. Continuous-time Dynamic Network Embeddings. In *Companion Proceedings of the Web Conference 2018*, 969–976.
- [34] Maximilian Nickel and Douwe Kiela. 2017. Poincaré Embeddings for Learning Hierarchical Representations. In *Advances in Neural Information Processing Systems*, I. Guyon, U. Von Luxburg, S. Bengio, H. Wallach, R. Fergus, S. Vishwanathan, and R. Garnett (Eds.), Vol. 30. Curran Associates, Inc. <https://proceedings.neurips.cc/paper/2017/file/59dfa2df42d9e3d41f5b02bfc3229dd-Paper.pdf>
- [35] Maximilian Nickel and Douwe Kiela. 2018. Learning Continuous Hierarchies in the Lorentz Model of Hyperbolic Geometry. In *Proceedings of the 35th International Conference on Machine Learning (Proceedings of Machine Learning Research, Vol. 80)*, Jennifer Dy and Andreas Krause (Eds.). PMLR, 3779–3788. <https://proceedings.mlr.press/v80/nickel18a.html>
- [36] Yann Ollivier. 2009. Ricci Curvature of Markov Chains on Metric Spaces. *Journal of Functional Analysis* 256, 3 (2009), 810–864.
- [37] Danilo Jimenez Rezende, George Papamakarios, Sébastien Racanière, Michael Alberg, Gurtej Kanwar, Phiala Shanahan, and Kyle Cranmer. 2020. Normalizing Flows on Tori and Spheres. In *International Conference on Machine Learning*. PMLR, 8083–8092.
- [38] Jayson Sia, Edmond Jonckheere, and Paul Bogdan. 2019. Ollivier-ricci Curvature-based Method to Community Detection in Complex Networks. *Scientific reports* 9, 1 (2019), 1–12.
- [39] Ondrej Skopek, Octavian-Eugen Ganea, and Gary Becigneul. 2020. Mixed-curvature Variational Autoencoders. In *International Conference on Learning Representations*. <https://openreview.net/forum?id=S1g6xeSKDS>
- [40] Rishi Sonthalia and Anna Gilbert. 2020. Tree! I am no Tree! I am a low dimensional Hyperbolic Embedding. In *Advances in Neural Information Processing Systems*, H. Larochelle, M. Ranzato, R. Hadsell, M.F. Balcan, and H. Lin (Eds.), Vol. 33. Curran Associates, Inc., 845–856. <https://proceedings.neurips.cc/paper/2020/file/093f65e080a295f80761c5722a46aa2-Paper.pdf>
- [41] RP Sreejith, Karthikeyan Mohanraj, Jürgen Jost, Emil Saucan, and Areejit Samal. 2016. Forman Curvature for Complex Networks. *Journal of Statistical Mechanics*:

- Theory and Experiment* 2016, 6 (2016), 063206.
- [42] Jianing Sun, Zhaoyue Cheng, Saba Zuberi, Felipe Perez, and Maksims Volkovs. 2021. HGCF: Hyperbolic Graph Convolution Networks for Collaborative Filtering. In *Proceedings of the Web Conference 2021* (Ljubljana, Slovenia) (WWW '21). Association for Computing Machinery, New York, NY, USA, 593–601. <https://doi.org/10.1145/3442381.3450101>
- [43] Li Sun, Junda Ye, Hao Peng, Feiyang Wang, and Philip S. Yu. 2023. Self-Supervised Continual Graph Learning in Adaptive Riemannian Spaces. In *Proceedings of the AAAI Conference on Artificial Intelligence*.
- [44] Li Sun, Junda Ye, Hao Peng, and Philip S. Yu. 2022. A Self-supervised Riemannian GNN with Time Varying Curvature for Temporal Graph Learning. In *Proceedings of the 31st ACM International Conference on Information & Knowledge Management*. 1827–1836.
- [45] Li Sun, Zhongbao Zhang, Junda Ye, Hao Peng, Jiawei Zhang, Sen Su, and Philip S. Yu. 2022. A Self-supervised Mixed-curvature Graph Neural Network. In *Proceedings of the AAAI Conference on Artificial Intelligence*, Vol. 36. 4146–4155.
- [46] Li Sun, Zhongbao Zhang, Jiawei Zhang, Feiyang Wang, Hao Peng, Sen Su, and Philip S. Yu. 2021. Hyperbolic Variational Graph Neural Network for Modeling Dynamic Graphs. In *Proceedings of the AAAI Conference on Artificial Intelligence*, Vol. 35. 4375–4383.
- [47] Abraham Albert Ungar. 2008. A Gyrovectorspace Approach to Hyperbolic Geometry. *Synthesis Lectures on Mathematics and Statistics* 1, 1 (2008), 1–194.
- [48] Abraham Albert Ungar. 2010. *Barycentric Calculus in Euclidean and Hyperbolic Geometry: A Comparative Introduction*. World Scientific.
- [49] Lucas Vinh Tran, Yi Tay, Shuai Zhang, Gao Cong, and Xiaoli Li. 2020. *HyperML: A Boosting Metric Learning Approach in Hyperbolic Space for Recommender Systems*. Association for Computing Machinery, New York, NY, USA, 609–617. <https://doi.org/10.1145/3336191.3371850>
- [50] Yiwei Wang, Yujun Cai, Yuxuan Liang, Henghui Ding, Changhu Wang, Sidharth Bhatia, and Bryan Hooi. 2021. Adaptive Data Augmentation on Temporal Graphs. In *Advances in Neural Information Processing Systems*, M. Ranzato, A. Beygelzimer, Y. Dauphin, P.S. Liang, and J. Wortman Vaughan (Eds.), Vol. 34. Curran Associates, Inc., 1440–1452. <https://proceedings.neurips.cc/paper/2021/file/0b0b0994d12ad343511adfbfc364256e-Paper.pdf>
- [51] Yanbang Wang, Yen-Yu Chang, Yunyu Liu, Jure Leskovec, and Pan Li. 2021. Inductive Representation Learning in Temporal Networks via Causal Anonymous Walks. In *International Conference on Learning Representations*. <https://openreview.net/forum?id=KYPz4YsCPJ>
- [52] Richard C Wilson, Edwin R Hancock, Elzbieta Pekalska, and Robert PW Duin. 2014. Spherical and Hyperbolic Embeddings of Data. *IEEE transactions on pattern analysis and machine intelligence* 36, 11 (2014), 2255–2269.
- [53] Chao-Yuan Wu, Amr Ahmed, Alex Beutel, Alexander J Smola, and How Jing. 2017. Recurrent Recommender Networks. In *Proceedings of the Tenth ACM International Conference on Web Search and Data Mining*. 495–503.
- [54] Da Xu, Chuanwei Ruan, Evren Korpeoglu, Sushant Kumar, and Kannan Achan. 2020. Inductive Representation Learning on Temporal Graphs. In *International Conference on Learning Representations*. <https://openreview.net/forum?id=rJeW1yHYwH>
- [55] Menglin Yang, Min Zhou, Marcus Kalander, Zengfeng Huang, and Irwin King. 2021. Discrete-Time Temporal Network Embedding via Implicit Hierarchical Learning in Hyperbolic Space. In *Proceedings of the 27th ACM SIGKDD Conference on Knowledge Discovery & Data Mining (Virtual Event, Singapore) (KDD '21)*. Association for Computing Machinery, New York, NY, USA, 1975–1985. <https://doi.org/10.1145/3447548.3467422>
- [56] Ze Ye, Kin Sum Liu, Tengfei Ma, Jie Gao, and Chao Chen. 2020. Curvature Graph Network. In *International Conference on Learning Representations*. <https://openreview.net/forum?id=BylEqnVFDB>
- [57] Yiding Zhang, Xiao Wang, Chuan Shi, Nian Liu, and Guojie Song. 2021. Lorentzian Graph Convolutional Networks. In *Proceedings of the Web Conference 2021*. 1249–1261.
- [58] Shichao Zhu, Shirui Pan, Chuan Zhou, Jia Wu, Yanan Cao, and Bin Wang. 2020. Graph Geometry Interaction Learning. *Advances in Neural Information Processing Systems* 33 (2020), 7548–7558.
- [59] Yu Zhu, Hao Li, Yikang Liao, Beidou Wang, Ziyu Guan, Haifeng Liu, and Deng Cai. 2017. What to Do Next: Modeling User Behaviors by Time-LSTM. In *Proceedings of the Twenty-Sixth International Joint Conference on Artificial Intelligence*, Vol. 17. 3602–3608.
- [60] Yuan Zuo, Guannan Liu, Hao Lin, Jia Guo, Xiaoqian Hu, and Junjie Wu. 2018. Embedding Temporal Network via Neighborhood Formation. In *Proceedings of KDD*. 2857–2866.